Superlattice k·p models for calculating electronic structure

N. F. Johnson, H. Ehrenreich,* and G. Y. Wu
Division of Applied Sciences, Harvard University, Cambridge, Massachusetts 02138

T. C. McGill
Thomas J. Watson, Sr., Laboratory of Applied Physics, California Institute of Technology, Pasadena, California 91125
(Received 6 July 1988)

A quantitative comparison is presented of two realistic superlattice **k·p** electronic structure calculations. The first is an analytic approach based on an extended bulk Kane model; the second is an extended-basis treatment, developed by McGill and collaborators, based on bulk pseudopotential calculations. Both approaches are applied to HgTe/CdTe superlattices. Energies, wave functions, effective masses, and oscillator strengths are found to agree within 10%. The limited-basis approach based on the Kane model is seen to be adequate for superlattices whose bulk constituents have direct gaps in the conduction- and valence-band regions near the superlattice band gap.

INTRODUCTION

The electronic properties of semiconductor superlattices are most conveniently calculated using the bulk electronic structures of the constituent materials obtained by the **k·p** method as a starting point.[1] In this approach,[2] the superlattice (SL) wave function for SL band L at wave vector $\mathbf{K}$ is expanded in terms of a Luttinger basis as

$$\langle \mathbf{r}|L,\mathbf{K}\rangle = \sum_n F_n(L,\mathbf{K};\mathbf{r})\langle \mathbf{r}|n\rangle ,$$

where $\langle \mathbf{r}|n, \mathbf{k}=\mathbf{0}\rangle \equiv \langle \mathbf{r}|n\rangle$ is the bulk Bloch function of band n at $\mathbf{k}=\mathbf{0}$. Both constituents will be regarded as direct-band-gap materials with valence-band maxima and conduction-band minima at $\mathbf{k}=\mathbf{0}$. $F_n(L,\mathbf{K};\mathbf{r})$ is the envelope function.[2]

The correct microscopic boundary conditions demand that at each interface $\langle \mathbf{r}|L,\mathbf{K}\rangle$ and its derivative be continuous for all $\mathbf{r}$. In practice, however, most calculations employ approximate boundary conditions which are obtained after averaging the SL wave function over a bulk unit cell. This practice derives from the fact that the bulk basis set $\{\langle \mathbf{r}|n\rangle\}$ must be truncated for tractable computations. The bulk band structure therefore must be chosen so as to include the most important physical features in their simplest form and the basis set must be sufficiently complete that the boundary conditions are satisfied to a suitable level of approximation.

This paper compares the results of two such calculations involving quite different levels of basis-set truncations. One model, developed by McGill and collaborators, to be termed the extended-basis model considers an extended basis containing 54 $\langle \mathbf{r}|n\rangle$'s.[3–5] The other simpler model, to be termed the limited-basis model, considers only the eight fold basis contained in the Kane model but yields analytic results.[2,6] It will be seen, in reference to the HgTe/CdTe SL, that the simpler approach is sufficient for a quantitative description of the SL electronic properties over the energy region subsumed by the lowest band gaps. At the same time we emphasize that for SL having constituents with indirect band gaps, or for properties (e.g., optical) involving larger energy ranges, a more elaborate approach, such as the extended-basis model, is required.

DESCRIPTION OF MODELS

We begin with a precise specification of the two models. The limited-basis model (LBM) considers only the eight $\langle \mathbf{r}|n\rangle$ in Eq. (1) that are contained in the bulk Kane model including spin-orbit splitting. A finite heavy-hole mass results from the inclusion of the antibonding conduction-band p state by perturbation theory. The LBM has been used successfully to calculate SL gaps,[2] effective masses[6] using the f sum rule, and the optical absorption coefficients in various III-V-compound and II-VI compound superlattices.[7]

Specifically, the features associated with the model are the following.

(1) The bulk band structures are assumed isotropic.

(2) The bulk **k·p** parameters are taken from experiment. This applies to the effective masses m^* and band gaps E_g for both constituents. The optical matrix elements $P_{nn'}=\langle n, \mathbf{k}=\mathbf{0}|\mathbf{p}|n', \mathbf{k}=\mathbf{0}\rangle$ are deduced from the Kane model and the experimental bulk m^* and E_g. The difference between the $P_{nn'}$ for HgTe and CdTe is less than 10%. A single value of $P_{nn'}$, applicable to either constituent, is obtained from an arithmetic mean.

(3) The $\langle \mathbf{r}|n\rangle$ are assumed the same for each constituent. The procedure for obtaining the parameters described in (2) is essentially equivalent to that assumption.

(4) Superlattice $\mathbf{K}=\mathbf{0}$ energies, masses, and envelope functions can be obtained analytically.

The extended-basis model[3–5] (EBM) contains many bands in addition to those considered within the Kane model. These bands are folded down using Löwdin perturbation theory. The EBM is properly regarded as the "state of the art" of the superlattice **k·p** approaches.

Specifically, the model contains the following features.

(1) The bulk band structure and the $\langle \mathbf{r}|n\rangle$ are obtained from an empirical pseudopotential calculation that contains the full zinc-blende symmetry.

(2) The bulk **k·p** parameters are calculated utilizing these pseudopotential results.

(3) The $\langle \mathbf{r}|n \rangle$, and hence the parameters calculated from them, differ for the two constituents, in contrast to the LBM.

(4) The boundary conditions, as expected, are better satisfied by the EBM than by the LBM.

The results for HgTe/CdTe obtained from each of these two approaches as described above will be compared by using the bulk band gaps and effective masses resulting from the pseudopotential calculations of the EBM as input for the LBM as a common base.

CRITIQUE OF THE LIMITED-BASIS MODEL

The possible shortcomings of the LBM should be considered before proceeding to a detailed comparison. There are three major points of criticism.

The first concerns the adequacy of the LBM bulk band structure and the limited number of bulk bands involved in the description. Figure 1 compares the bulk band structure as a function of complex $\mathbf{k}$ for $Hg_{0.5}Cd_{0.5}Te$ for the two models in the virtual crystal approximation. (This bulk band structure is appropriate here since the SL to be considered have equal layer widths.) The results agree well near $\mathbf{k}=\mathbf{0}$. For finite real $\mathbf{k}$, the LBM light hole band (Γ_8) flattens out too rapidly, as does the split-off band (Γ_7) along the Im($\mathbf{k}$) direction. These discrepancies are associated with the absence of higher and lower bulk bands in the LBM. For example, in the case of the split-off band (Γ_7) along Im($\mathbf{k}$) the higher band to which it connects is missing in the LBM. By contrast, since Γ_8 and Γ_6 are present in both models, the curvature along Im($\mathbf{k}$) is very similar in the two cases. These differences are of little concern even in a narrow layer width SL, since for the SL Brillouin zone of the (13 Å HgTe)/(13 Å CdTe) SL, demonstrated by a dotted vertical line in Fig. 1, and for the same region along the Im($\mathbf{k}$) axis the two sets of results are in very good agreement.

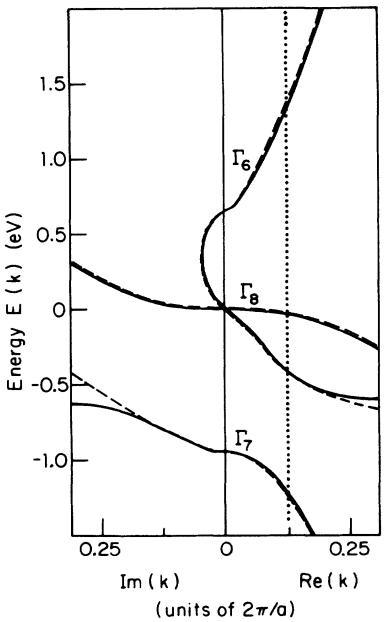

FIG. 1. Virtual crystal $Hg_{0.5}Cd_{0.5}Te$ bulk band structure $E(k)$ for a limited-basis (LBM—solid line) and extended-basis (EBM—dashed line) model vs real k and imaginary k; k is in units of $2\pi/a$, where a is bulk lattice constant. EBM calculation is for k parallel to [100]. Dotted vertical line denotes Brillouin-zone boundary for (13 Å HgTe)/(13 ÅCdTe) SL.

The consequences of neglecting the full zinc-blende symmetry, as exemplified by the choice of different growth axes, are discussed in Ref. 4. The differences are on the meV scale, and are smaller than those resulting from the neglect of basis states in the LBM.

The second concern is the assumption that the $\langle \mathbf{r}|n \rangle$ are the same for each SL constituent. This assumption implies that the $P_{nn'}$ are material independent in the LBM description of the superlattice. The substantial constancy of direct gap momentum matrix elements in the III-V compound and II-VI compound bulk semiconductors has been long recognized and is by now well documented.[1,8] However, this assumption, while certainly valid for HgTe/CdTe, requires reexamination for superlattices whose constituents involve different rows of the Periodic Table. These assertions are supported also by the pseudopotentials given in the review by Cohen and Heine.[9]

The third question concerns the interface boundary conditions and whether they are adequately satisfied in the LBM. The current averaged over a bulk unit cell is continuous across the interface for both models considered in this paper at $\mathbf{K}=\mathbf{0}$. However, the extent to which the microscopic boundary conditions are satisfied in the LBM because of the more severe basis-set truncations and the neglect of pseudo-wave-function differences requires detailed examination. This matter will be discussed in the next section. The implementation of the LBM boundary conditions is equivalent to that in Refs. 2 and 10, while that of the EBM is equivalent to that described in Ref. 4.

DETAILED COMPARISON

HgTe/CdTe is a type-III superlattice because of the inverted bulk band structure of HgTe. The *s-p* mixing accordingly is much larger than that characteristic of the wide gap type-I superlattices, many (but not all) of whose features can be described by the continuum approximation exemplified by the Kronig-Penney model. The strong *s-p* admixture in the SL under consideration amplifies the difficulty of satisfying the boundary conditions. The situation is made yet more difficult in the thin-layer limit, to be considered here, in which the interface region comprises a significant fraction of the SL period. Strain effects will be neglected because the superlattice under consideration is well lattice matched.

The (13 Å HgTe)/(13 Å CdTe) SL contains only eight molecular layers per period. The results for the envelope functions to be presented assume a valence band offset of 40 meV. While this value is now widely believed to be too small, the quantitative aspects of the comparison made here are little affected by the choice of a larger offset.

The unit-cell average used in obtaining the approximate boundary conditions implies that they can be expressed entirely in terms of the envelope functions

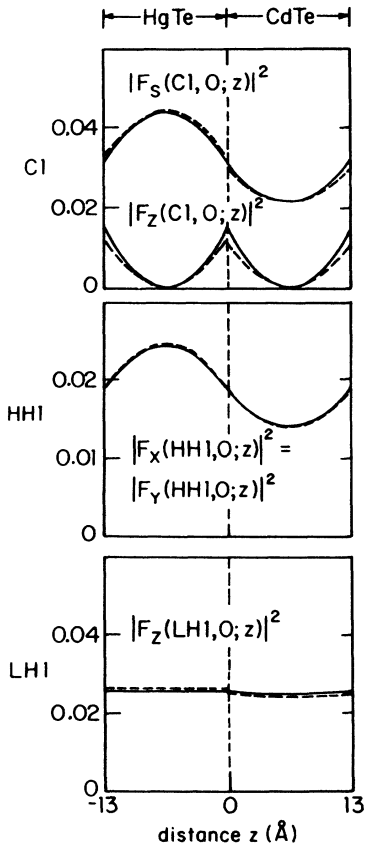

FIG. 2. Square of absolute value of dominant envelope functions vs distance along growth (z) axis for the $\mathbf{K}=0$ (13 Å HgTe)/(13 Å CdTe) superlattice states for superlattice bands C1, HH1, and LH1. Solid and dashed lines correspond to limited-basis and extended-basis models, respectively. The superlattice wave function is normalized to unity over the 26-Å period.

$F_n(L,\mathbf{K};z)$. These correspond to the bulk basis states [cf. Eq. (1)] $|n\rangle=|S\rangle$, $|X\rangle$, $|Y\rangle$, and $|Z\rangle$ in the notation of Ref. 1 or equivalently to the linear combinations appropriate to the band edges under consideration as defined by Kane.

Figure 2 shows the most important $|F_n(L,0;z)|^2$ for the (13 Å HgTe)/(13 Å CdTe) SL as a function of distance along the growth axis on either side of the HgTe/CdTe interface, which is taken to correspond to $z=0$. The envelope functions shown correspond to the conduction-band minimum ($L=$C1) and the bands nearest the valence-band maximum ($L=$LH1, light-hole band; $L=$HH1, heavy-hole band). In both models the envelope functions are continuous to a good approximation. The discontinuities in the $|F_n(L,0;z)|^2$ are seen to be larger for the EBM. This discrepancy is only apparent: The continuity conditions apply to quantities involving $F_n(L,0;z)\langle \mathbf{r}|n\rangle$, and are still satisfied within the EBM since the difference between the $\langle \mathbf{r}|n\rangle$ on either side of the interface in the EBM compensates for the discontinuity in the F_n. The magnitude of the two sets of F_n are in excellent overall agreement. Significant differences extend over only a small region of the distance $z=26$ Å shown in the figure. For a (39 Å HgTe)/(39 Å CdTe) superlattice that region becomes a smaller fraction of the total. Properties, such as optical matrix elements and tunneling probabilities, depending only on integrals involving the F_n will therefore be well described in both approximations.[11] $|F_Z(C1,0;z)|^2$ exhibits evanescent character, as does $|F_Z(LH1,0;z)|^2$ to a lesser extent. (LH1 is commonly termed the "interface state" for that reason.) The HH1 envelope function is seen to be more confined within the HgTe layer than the LH1 function. This is because the bulk heavy-hole mass is larger than the bulk light-hole mass, and hence the tunneling probability out of the HgTe layer (which acts as the quantum well for the hole states) is smaller for the heavy hole than for the light hole. This effect is amplified if the band offset is made larger.

Table I compares energies, masses, and oscillator strengths for (13 Å HgTe)/(13 Å CdTe) and (39 Å HgTe)/(39 Å CdTe) superlattices, as given by the LBM and EBM. $E_L(0)$ is the $\mathbf{K}=0$ energy of SL band L, $m_L^{\perp}$ is the corresponding effective mass perpendicular to the layers, and $f^{\parallel}_{\mathrm{VB,C1}}$ is the total $\mathbf{K}=0$ oscillator strength (polarization parallel to the layers) between the superlattice valence bands LH1 and HH1, and C1. The agreement of $m_L^{\perp}$ and $f^{\parallel}_{\mathrm{VB,C1}}$ illustrates the ability of the LBM to predict superlattice properties analytically both perpendicular *and* parallel to the layers.[12] (References 2 and 4

TABLE I. Comparison of superlattice energies $E_L(0)$, masses $m_L^{\perp}$ perpendicular to the planes, and total valence-band to conduction-band oscillator strengths $f^{\parallel}_{\mathrm{VB,C1}}$, where polarization is parallel to the planes for (13 Å HgTe)/(13 Å CdTe), and (39 Å HgTe)/(39 Å CdTe) superlattices as calculated in the limited-basis (LBM) and extended-basis (EBM) models. m_0 is the free-electron mass.

	(13 Å HgTe)/(13 Å CdTe)		(39 Å HgTe)/(39 Å CdTe)	
	EBM	LBM	EBM	LBM
$E_{\mathrm{C1}}(0)$ (eV)	0.48	0.50	0.21	0.23
$E_{\mathrm{HH1}}(0)$ (eV)	−0.018	−0.018	−0.0085	−0.0095
$E_{\mathrm{LH1}}(0)$ (eV)	−0.020	−0.019	−0.019	−0.019
$m^{\perp}_{\mathrm{C1}}$	$0.050m_0$	$0.047m_0$	$0.092m_0$	$0.099m_0$
$m^{\perp}_{\mathrm{HH1}}$	$-1.1m_0$	$-1.0m_0$	∞	∞
$m^{\perp}_{\mathrm{LH1}}$	$-0.055m_0$	$-0.052m_0$	$-0.055m_0$	$-0.058m_0$
$f^{\parallel}_{\mathrm{VB,C1}}$	21	20	27	26

speculate that parallel properties, e.g., $f^{\Downarrow}_{VB,C1}$ would not be reliably given within the Kane model without extensive numerical computation.) The agreement between the models for a given layer thickness is generally better for the hole states (LH1, HH1) than for the electron state (C1). This is a consequence of the small valence-band offset which causes the hole states to lie in an energy region where the bulk band structures of the constituent materials are well described by both models, i.e., close to $\mathbf{k}=\mathbf{0}$. (This conclusion will not be appreciably modified for offsets as large as 350 meV.)

Since the HgTe/CdTe case considered here is one in which the LBM is put to a particularly stringent test, one would expect this model to be applicable to other SL as well. This observation is confirmed by our experience.[6,7]

ACKNOWLEDGMENTS

This work was supported by the Joint Services Electronics Program through U.S. Office of Naval Research (ONR) Contract No. N00014-84-K-0465, and by the Defense Advanced Research Projects Agency through ONR Contracts Nos. N00014-86-K-0033, N00014-86-K-0760, and N00014-86-K-0841.

---

*To whom all correspondence should be addressed.

[1]E. O. Kane, in *Narrow Gap Semiconductors: Physics and Applications,* Vol. 133 of Lecture Notes in Physics, edited by W. Zawadzki (Springer-Verlag, New York, 1981), p. 13.

[2]G. Bastard, in *Proceedings of the NATO Advanced Study Institute on Molecular Beam Epitaxy in Heterostructures, Erice, Italy, 1983,* edited by L. L. Chang and K. Ploog (Martinus-Nijhoff, Dordrecht, 1984), p. 381. See also, G. Bastard, Phys. Rev. B **25**, 7584 (1982).

[3]C. Mailhiot, T. C. McGill, and D. L. Smith, J. Vac. Sci. Technol. B **2**, 371 (1984).

[4]D. L. Smith and C. Mailhiot, Phys. Rev. B **33**, 8345 (1986).

[5]C. Mailhiot and D. L. Smith, Phys. Rev. B **33**, 8360 (1986).

[6]N. F. Johnson, H. Ehrenreich, K. C. Hass, and T. C. McGill, Phys. Rev. Lett. **59**, 2352 (1987).

[7]N. F. Johnson, H. Ehrenreich, and R. V. Jones, Appl. Phys. Lett. **53**, 180 (1988).

[8]H. Ehrenreich, J. Appl. Phys. **32**, 2155 (1961).

[9]M. L. Cohen and V. Heine, in *Solid State Physics,* edited by H. Ehrenreich, F. Seitz, and D. Turnbull (Academic, New York, 1970), Vol. 24, p. 37.

[10]R. I. Taylor and M. G. Burt, Semicond. Sci. Technol. **2**, 485 (1987).

[11]This applies to the optical matrix element involving dF_n/dz, as we have verified, if the discontinuity at the interface is neglected or a suitable "smoothing function" is introduced.

[12]Although the present comparison involves $\mathbf{K}=\mathbf{0}$ quantities, the LBM does successfully predict finite-$\mathbf{K}$ properties using superlattice $\mathbf{K}\cdot\mathbf{p}$ perturbation theory. See N. F. Johnson, P. M. Hui, and H. Ehrenreich, Phys. Rev. Lett. (to be published).